



Published in final edited form as:

*Cell Host Microbe*. 2010 December 16; 8(6): 484–495. doi:10.1016/j.chom.2010.11.005.

## Phosphorylation of immunity-related GTPases by a *Toxoplasma gondii* secreted kinase promotes macrophage survival and virulence

Sarah J. Fentress<sup>1</sup>, Michael S. Behnke<sup>1</sup>, Ildiko R. Dunay<sup>1,\*</sup>, Mona Mashayekhi<sup>1</sup>, Leah M. Rommereim<sup>2</sup>, Barbara A. Fox<sup>2</sup>, David J. Bzik<sup>2</sup>, Gregory A. Taylor<sup>3</sup>, Benjamin E. Turk<sup>4</sup>, Cheryl F. Lichti<sup>5</sup>, R. Reid Townsend<sup>5,6</sup>, Wei Qiu<sup>7</sup>, Raymond Hui<sup>7</sup>, Wandy L. Beatty<sup>1</sup>, and L. David Sibley<sup>1,\*\*</sup>

<sup>1</sup> Department of Molecular Microbiology, Washington University School of Medicine, 660 S. Euclid Ave, St. Louis, MO 63130

<sup>2</sup> Department of Microbiology and Immunology, Dartmouth School of Medicine, Lebanon, NH, 03756

<sup>3</sup> Departments of Medicine, Molecular Genetics and Microbiology, and Immunology, Division of Geriatrics, and Center for the Study of Aging and Human Development, Duke University Medical Center, Durham, NC 27710; Geriatric Research, Education, and Clinical Center, VA Medical Center, Durham, NC 27705

<sup>4</sup> Department of Pharmacology, Yale University School of Medicine, 333 Cedar St., New Haven, CT, 06520

<sup>5</sup> Department of Medicine, Washington University School of Medicine, 660 S. Euclid Ave, St. Louis, MO 63130

<sup>6</sup> Department of Cell Biology and Physiology, Washington University School of Medicine, 660 S. Euclid Ave, St. Louis, MO 63130

© 2010 Elsevier Inc. All rights reserved.

\*\* Corresponding author: sibley@wustl.edu, TEL: 314-362-8873, FAX: 314-286-0060.

\* Present address: Department of Neuropathology, University of Freiburg, Breisacherstrasse 64, Freiburg, Germany, 79106

### AUTHOR CONTRIBUTIONS

S.J.F. designed and performed the majority of experiments, analyzed the data, generated the figures and contributed to writing the manuscript. I.R.D. and M.M. assisted with the *in vivo* experiments and performed the flow cytometry analysis, M.S.B. and B.E.T. performed the motif analyses, L.M.R., B.A.F., and D.J.B. generated and validated the *Δrop18* knockout, W.L.B. performed the EM experiments, G.A.T. provided key reagents and insight into IRG function, W.Q., R.H., C.F.L., and R.R.T. performed the MS experiments, L.D.S. supervised the studies, contributed to design and analyses of the experiments, and writing / editing of the manuscript. All authors approved the manuscript.

**Publisher's Disclaimer:** This is a PDF file of an unedited manuscript that has been accepted for publication. As a service to our customers we are providing this early version of the manuscript. The manuscript will undergo copyediting, typesetting, and review of the resulting proof before it is published in its final citable form. Please note that during the production process errors may be discovered which could affect the content, and all legal disclaimers that apply to the journal pertain.

### HIGHLIGHTS

- The secreted *Toxoplasma gondii* kinase ROP18 protects parasites from macrophage killing
- The host factor Irgb6 is required for efficient parasite killing by macrophages
- ROP18 phosphorylates IRG family members within a conserved domain
- ROP18 is necessary and sufficient to block IRG vacuolar accumulation

### SUPPLEMENTAL INFORMATION

Supplementary information includes six figures, four tables, one data file, and supplemental Experimental Procedures that can be found at:

<sup>7</sup> Structural Genomics Consortium, University of Toronto, MaRS South Tower, Suite 732, 101 College Street, Toronto Ontario Canada M5G 1L7

## SUMMARY

Macrophages are specialized to detect and destroy intracellular microbes and yet a number of pathogens have evolved to exploit this hostile niche. Here we demonstrate that the obligate intracellular parasite *Toxoplasma gondii* disarms macrophage innate clearance mechanisms by secreting a serine threonine kinase called ROP18, which binds to and phosphorylates immunity-related GTPases (IRGs). Substrate profiling of ROP18 revealed a preference for a conserved motif within switch region I of the GTPase domain, a modification predicted to disrupt IRG function. Consistent with this, expression of ROP18 was both necessary and sufficient to block recruitment of Irgb6, which was in turn required for parasite destruction. ROP18 phosphorylation of IRGs prevented clearance within inflammatory monocytes and IFN- $\gamma$ -activated macrophages, conferring parasite survival *in vivo* and promoting virulence. IRGs are implicated in clearance of a variety of intracellular pathogens, suggesting that other virulence factors may similarly thwart this innate cellular defense mechanism.

## INTRODUCTION

*Toxoplasma gondii* can infect virtually all warm-blooded vertebrates by actively invading nucleated host cells and forming a modified compartment known as the parasitophorous vacuole (PV) (Sibley, 2004). This niche provides a safe haven for replication and avoids clearance mechanisms in resting cells, including professional phagocytes such as monocytes/macrophages (Sibley et al., 2007). In contrast, IFN- $\gamma$  activated cells are able to either directly kill the parasite or induce stasis (Yap et al., 2006). Prominent among the control mechanisms of activated cells is upregulation of a family of immunity-related GTPases (IRGs) (Martens and Howard, 2006), which clear the parasite by rupturing the vacuole, resulting in parasite degradation (Taylor et al., 2007). IRGs are implicated in resistance to a variety of intracellular pathogens including *Chlamydia*, *Mycobacteria*, *Leishmania*, *Listeria*, and *Salmonella* (Taylor et al., 2007). Although the mechanism by which IRGs destroy intracellular pathogens is uncertain, they cycle between GDP-GTP bound forms, slowly hydrolyze GTP, and cooperatively oligomerize in the GTP-bound conformation on the surface of *T. gondii*-containing vacuoles (Hunn et al., 2008). IRGs contain a conserved GTPase domain and an extensive N-terminal helical region, which groups them with the dynamin family of GTPases (Ghosh et al., 2004). Clearance of *T. gondii* involves sequential recruitment of multiple IRGs onto the parasite-containing vacuole membrane and culminates in parasite destruction within ~ 2 h of infection (Ling et al., 2006; Martens et al., 2005; Zhao et al., 2009b). Most strains of *T. gondii* belong to one of three prominent lineages, which differ dramatically in acute virulence in the mouse model (Sibley and Ajioka, 2008), and in susceptibility to IRG-mediated clearance. Virulent type I strains resist recruitment and avoid clearance, while less virulent type II and III strains are effectively cleared by IRGs (Khaminets et al., 2010; Zhao et al., 2009a).

Forward genetic screens have revealed that virulence differences between strains of *T. gondii* are largely mediated by the highly polymorphic serine threonine (S/T) kinase ROP18, which is expressed at a much lower level in type III strains compared to types I and II (Saeij et al., 2006; Taylor et al., 2006). ROP18 belongs to a unique family of kinases that have been amplified in the parasite by recent gene duplication and diversification (Peixoto et al., 2010). During host cell invasion, the parasite secretes ROP18 into the host cell cytosol in small vesicles derived from apical secretory organelles called rhoptries (Håkansson et al., 2001; Taylor et al., 2006). ROP18 is subsequently targeted to the external surface of the parasite-containing vacuole, where its kinase activity is essential for virulence (Taylor et al.,

2006). Transgenic expression of ROP18 from a type I lineage in the avirulent type III strain results in rapid death in the mouse following low dose challenge, recapitulating the phenotype of the type I lineage (Taylor et al., 2006). Although progress has been made in understanding the structure (Labesse et al., 2009; Qiu et al., 2008), regulation (Qiu et al., 2008), cellular trafficking (Labesse et al., 2009; Reese and Boothroyd, 2009), and evolution (Khan et al., 2009) of ROP18, the mechanism by which it enhances virulence remains unknown.

Infection by *T. gondii* stimulates recruitment of inflammatory monocytes, a subset of bone-marrow-derived cells that express Gr1 (Ly6C) and CCR2, allowing them to home to sites of inflammation (Geissmann et al., 2010). Inflammatory monocytes are essential for clearance of *T. gondii* early after infection in the mouse either following i.p. inoculation (Mordue and Sibley, 2003; Robben et al., 2005) or oral infection (Dunay et al., 2008). Among their effector functions, macrophages upregulate IRGs and recruit them to the parasite-containing vacuole via an Atg5-dependent pathway that does not involve lysosomal fusion (Zhao et al., 2008), and which is independent of iNOS produced nitric oxide (Zhao et al., 2009a). Given the critical importance of ROP18 in acute virulence, we examined parasite survival within Gr1<sup>+</sup> monocytes. These studies reveal a mechanism whereby ROP18 phosphorylates IRGs and blocks their ability to eliminate intracellular parasites.

## RESULTS

### ROP18 mediates survival within inflammatory monocytes

Expression of ROP18 derived from a type I strain in the type III lineage decreases the lethal dose by > 4 logs and yet only modestly alters growth rate *in vitro* (Taylor et al., 2006), suggesting that ROP18 imparts a particular survival advantage *in vivo*. Consistent with this, dramatic differences in the expansion of strains were evident within the peritoneal cavity following low inoculum infection and this was strictly correlated with ROP18 expression (Figure 1A). Type I parasites (ROP18 expressing) underwent rapid expansion, while type III (ROP18-deficient) remained at background levels (Figure 1A). This difference in expansion was recapitulated with a slight lag phase in mice infected by transgenic type III parasites expressing an active form of ROP18 (Type III + ROP18), but not a kinase-dead form of the enzyme (Type III + ROP18 D/A) (Figure 1A). The dramatic difference in expansion *in vivo*, which occurs in the absence of a comparable difference in intrinsic growth rates (Taylor et al., 2006), suggests that ROP18 imparts a unique ability to survive within cells in the peritoneum.

Infection with *T. gondii* normally elicits recruitment of inflammatory monocytes (Gr1<sup>+</sup> F4/80<sup>+</sup>), which are equipped with several mechanisms for parasite clearance including iNOS expression, TNF- $\alpha$  secretion, and IL-12 production (Dunay et al., 2008; Mordue and Sibley, 2003; Robben et al., 2005). Infection with different strains of *T. gondii* elicited Gr1<sup>+</sup> monocyte recruitment to the peritoneum, and the number of monocytes was strongly correlated with parasite expansion, being highest in mice infected with type I strains and type III parasites expressing active ROP18 (Figure 1 B,C). Although resident macrophages (Gr1<sup>-</sup> F4/80<sup>+</sup>) were also infected (data not shown), high numbers of parasites were found within inflammatory monocytes (Figure 1 D,E).

The rapid expansion of ROP18-expressing parasites within inflammatory monocytes is surprising given the previously demonstrated microbicidal activity of these cells (Dunay et al., 2008; Mordue and Sibley, 2003; Robben et al., 2005). To examine the ability of *T. gondii* strains to survive within inflammatory monocytes, Gr1<sup>+</sup> F4/80<sup>+</sup> cells were elicited by low-level infection with type III parasites, which recruit monocytes but do not expand *in vivo*. Elicited Gr1<sup>+</sup> monocytes were tested *in vitro* for their ability to clear parasite infection

using an assay that monitors the % of infected cells over time and which is independent of parasite replication (Figure S1A). Gr1<sup>+</sup> monocytes efficiently cleared ROP18-deficient parasites *in vitro* while parasites expressing active ROP18 resisted destruction (Figure 1F). Similar ROP18 dependent survival was observed in unstimulated resident peritoneal macrophages (i.e. naïve) and macrophages that were activated *in vitro* with IFN- $\gamma$  (Figure S1B). Collectively, these studies demonstrate that ROP18 allows the parasite to establish a critical foothold within inflammatory monocytes early in infection.

### **ROP18 avoids clearance by blocking recruitment of Irgb6**

*Toxoplasma* is normally able to survive within macrophages by avoiding lysosome fusion (Sibley et al., 2007). Hence, we examined the fate of intracellular parasites in Gr1<sup>+</sup> monocytes. Enhanced clearance of ROP18-deficient parasites was not associated with increased delivery to lysosomes as shown by the absence of staining with LAMP1 (data not shown). EM examination revealed that the majority of parasites expressing the active ROP18 (Type I and Type III + ROP18) resided within intact vacuoles, while those deficient in ROP18 (Type III and Type III + ROP18 D/A) were associated with a highly scalloped vacuole membrane that underwent rupture, leading to digestion of the parasite (Figure 2). Similarly, ROP18 expressing parasites survived within intact vacuoles while ROP18-deficient parasites underwent vacuole disruption and digestion in naïve and IFN- $\gamma$ -activated macrophages (Figure S2).

The cellular features of parasite clearance in inflammatory monocytes were reminiscent of IRG-mediated destruction described previously (Ling et al., 2006; Martens et al., 2005; Zhao et al., 2008). Therefore, we evaluated the recruitment of IRGs to the parasite-containing vacuole based on the protein Irgb6, which is an early sentinel of this process (Khaminets et al., 2010; Zhao et al., 2009b). Parasites expressing active ROP18 largely resisted IRG recruitment, while efficient Irgb6 loading was observed on vacuoles containing parasites deficient in ROP18 (Figure 3A,B). The level of ROP18 on the vacuole surrounding transgenic type III parasites expressing ROP18 was inversely correlated with Irgb6 staining, suggesting that high levels of ROP18 blocked recruitment (Figure S3A). Similarly, expression of active ROP18 was associated with disruption of Irgb6 recruitment and avoidance of clearance maintenance within naïve and IFN- $\gamma$  activated macrophages (Figures S3 B,C). Cryoimmuno-EM analysis revealed that Irgb6 was deposited directly on the vacuolar membrane, as well as being strongly concentrated on membranes in the region of the parasite-containing vacuole (Figure 3C, Figure S3 D-F). Collectively, these studies indicate that active ROP18 prevents recruitment of Irgb6 to the parasite-containing vacuole, thus providing an explanation for the failure of macrophages to clear parasites that express this parasite kinase.

### **ROP18 co-precipitates and directly phosphorylates IRGs**

During host cell invasion, ROP18 is secreted into the host cell cytosol and targeted to the external surface of the parasite-containing vacuole membrane (Taylor et al., 2006). This interface is largely devoid of host cell proteins due to the nonfusigenic nature of the vacuole (Sibley et al., 2007). In contrast, several IRGs are actively recruited to the parasite-containing vacuole membrane (Hunn et al., 2008; Ling et al., 2006; Martens et al., 2005; Zhao et al., 2009a), placing them on the same membrane interface with ROP18. Target selectivity of S/T kinases is often influenced by proximity (Hanks and Hunter, 1995), suggesting that ROP18 might phosphorylate IRGs, possibly altering their function and cellular trafficking. To provide biochemical evidence for such a process, Irgb6 was immunoprecipitated from infected cells and probed by Western blot, revealing a weak but detectable interaction with ROP18 (Figure 4A). The strength of this interaction was increased by 3-fold, as shown by phosphorimager analysis, in parasites expressing the

kinase-dead ROP18 D/A (Figure 4A), consistent with it being trapped with its substrate when unable to complete the phospho-transfer reaction. When ROP18 and Irgb6 were each separately immunoprecipitated and incubated *in vitro* in a hot kinase reaction, both auto-phosphorylation of several forms of ROP18 and labeling of Irgb6 were readily detected by the active ROP18 but not the kinase-dead form (Figure 4B). Finally, ROP18-dependent phosphorylation of Irgb6 was detected by orthophosphate-labeling and immunoprecipitation from cells infected with parasites expressing active but not kinase-dead ROP18 (Figure 4C), confirming that this modification also occurs *in vivo*. ROP18 was also co-immunoprecipitated from infected cell lysates with two other IRGs, Irga6 and Irgb10 (Figure 4 D, E), which are recruited to the *T. gondii* PV and implicated in pathogen clearance (Khaminets et al., 2010; Zhao et al., 2009a). Active ROP18 was also able to strongly phosphorylate Irga6 and Irgb10 *in vitro* when the proteins were separately immunoprecipitated and mixed together in a hot kinase reaction (Figure 4 F,G). Parasite expression of ROP18 was associated with avoidance of recruitment of Irga6 and Irgb10 in Gr1<sup>+</sup> monocytes (Fig. S4), similar to the results reported above for Irgb6. Collectively, our findings indicate ROP18 binds to and phosphorylates IRGs, likely preventing their accumulation on the parasite-containing vacuole and blocking parasite clearance.

### ROP18 targets a conserved motif in SWI of IRGs

To explore the target preference of ROP18, we performed *in vitro* phosphorylation assays using a positional-scanning peptide array (Turk et al., 2006). ROP18 showed a strong preference for Thr over Ser, and for Thr at multiple positions (Figure 5A). Conversion of the phosphopeptide blots to a sequence-based WebLogo revealed a slight preference for acidic residues upstream, and bulky hydrophobic residues downstream of the phosphorylation site (Figure 5B). To explore possible sites of phosphorylation, we analyzed a subset of IRGs that have previously been implicated in resistance to *T. gondii* (Figure 5C, Supplementary data file 1), for potential residues matching the ROP18 preference. MEME analysis identified potential sites that correspond to several well-characterized GTPase motifs including switch region I (SWI), switch region II (SWII), and N/TKxD (Figure S5 A,B), as described previously (Ghosh et al., 2004). Among these, SWI was the most highly scoring motif among all these IRG proteins and therefore we focused on this in subsequent analyses (Figure 5D, Figure S5 A,B). Consistent with this prediction, ROP18 was able to phosphorylate several Thr residues within a peptide derived from SWI of Irgb6 when tested *in vitro* (Figure 5E). The primary residue that was phosphorylated corresponded to GAAPTp, although less efficient modification was also detected for either of the residues within the sequence ETpTpMK (Figure S5 C,D). To verify that the same residues were modified within the intact protein, we analyzed phosphorylation of recombinant Irgb6 by ROP18 *in vitro* (Figure S5 E, supplemental Experimental Procedures). The tandem MS analysis of tryptic peptides confirmed that the GAAPTp sequence was phosphorylated (Figure 5F, S5F, Table S1); however, no other phosphopeptides were detected in the protein. Taken together, these studies demonstrate that ROP18 efficiently phosphorylates several IRGs *in vitro* and that it has a preference for a conserved site within SWI.

### ROP18 is necessary for macrophage survival

To test whether ROP18 was necessary for macrophage survival, we generated a clean deletion of *ROP18* in a type I background disrupted for nonhomologous end joining (so called  $\Delta ku80$  mutants) (Fox et al., 2009) (Figure S6 A-D). Examination of ROP18 expression by Western blotting revealed that the protein was no longer detectable (Figure 6A). As expected  $\Delta rop18$  parasites were less virulent in mice, while the parental  $\Delta ku80$  line retained full virulence (Figure 6B). Enhanced recruitment of Irgb6 to vacuoles containing  $\Delta rop18$  parasites occurred within IFN- $\gamma$ -activated macrophages, indicating that in the absence of ROP18, type I parasites are less able to avoid IRG recruitment (Figure 6C). The

*Δrop18* parasites were also more susceptible to clearance in naïve and IFN- $\gamma$ -activated peritoneal macrophages, as well as IFN- $\gamma$ -activated RAW 264.7 macrophages (Figure S6 E-G), demonstrating that ROP18 is important for survival in a variety of macrophage types. Although significant, the magnitude of the virulence and clearance defects in *Δrop18* parasites were less dramatic than seen for type III strains, supporting a role for other type I genes in contributing to differences in pathogenesis.

### Irgb6 recruitment is necessary for maximal clearance of parasites

Irgb6 is one of the first IRGs recruited to the PV (Khaminets et al., 2010), yet its role in pathogen clearance has not been directly tested owing to a lack of genetic knockouts for this gene, which is duplicated in the mouse genome (Zhao et al., 2009c). To test the requirement of Irgb6 in clearance, we down-regulated expression using specific siRNA constructs targeting both copies of Irgb6, resulting in 70% reduction of expression at the population level (Figure S6H). Shutdown was nearly complete in ~ 75% of cells, while a minority of cells were unaffected (Figure 6D,E). The enhanced clearance of *Δrop18* parasites that was observed in naïve and activated RAW macrophages was completely reversed in those cells where RNAi shutdown of Irgb6 was effective (Figure 6F, S6I). In addition, RNAi shutdown of Irgb6 in IFN- $\gamma$  activated RAW cells resulted in increased survival of type III parasite not expressing ROP18 (Figure S6J). In contrast, control siRNA had no effect on clearance (Figure 6D-F, S6H-J). Collectively, these studies demonstrate that ROP18 is both necessary and sufficient to avoid Irgb6 recruitment and promote survival in activated macrophages, while also establishing a critical role for Irgb6 in pathogen clearance.

## DISCUSSION

Previous genetic studies have shown that ROP18 mediates the major virulence differences between *T. gondii* strains (Saeij et al., 2006; Taylor et al., 2006), yet the mechanism of this enhanced pathogenicity remained unknown. We now demonstrate that ROP18 binds to and phosphorylates an important family of innate mediators called immunity related GTPases (IRGs), which are required for control of intracellular pathogens. Expression of ROP18 was associated with avoidance of IRG recruitment and survival in macrophages. Co-immunoprecipitation and *in vitro* labeling studies revealed that ROP18 directly phosphorylates IRGs, altering their cellular trafficking and function. The protective effect of ROP18 was observed in a variety of macrophage types including *in vitro* cell lines, naïve peritoneal cells, and IFN- $\gamma$ -activated macrophages. Most significantly, ROP18 had a strong protective effect in inflammatory monocytes, which home to the site of infection and are critical for control of parasite expansion (Dunay et al., 2008; Robben et al., 2005). Although previous reports have indicated that over-expression of ROP18 in the type I background enhances parasite growth (El Hajj et al., 2007), differences in replication rate do not appreciably contribute to the phenotypic differences between ROP18 expressing *vs.* deficient type III parasites (Taylor et al., 2006); hence the results reported here are primarily due to the ability of ROP18 to promote avoidance of clearance by the IRG system. Survival in this niche during early infection was associated with very rapid expansion, ultimately leading to death. Collectively our studies reveal that phosphorylation of IRGs by ROP18 results in survival in macrophages, thus revealing the molecular mechanism for its virulence enhancing activity.

IRG proteins are expressed at low levels in resting cells and strongly upregulated following exposure to IFN- $\gamma$  (Taylor et al., 2007). Previous studies using knockout mice have shown that several IRGs are important for control of intracellular *T. gondii*, including Irgm1 (LRG-47), Irgm3 (IGTP), Irgd (IRG-47), and Irga6 (IIGP-1) (Taylor et al., 2007). The current model for IRG function suggests that they load sequentially on the parasite-containing vacuole and effect membrane dissolution, by a yet uncharacterized means

(Khaminets et al., 2010). *Irgb6* and *Irgb10* are early markers of vacuoles that are destined for destruction and they show strain-specific recruitment correlated with clearance (Khaminets et al., 2010). Our study extends these findings by demonstrating that not only is *Irgb6* differentially recruited, it is necessary for efficient clearance of parasites in macrophages. Our studies demonstrate that the phosphorylation of *Irgb6*, and likely other IRGs, is associated with prevention of loading onto the vacuole, thus protecting the parasite from this clearance mechanism.

Although our data conclusively demonstrate that ROP18 prevents clearance in activated macrophages and inflammatory monocytes, other studies have reported that ROP18 is not sufficient for survival in macrophages isolated from mice immunized with an attenuated strain of *T. gondii* (Zhao et al., 2009a). The inability of transgenic type III strains expressing ROP18 to survive in macrophages from immunized mice is consistent with a heightened capacity to clear a type I parasite challenge *in vivo*, as shown previously (Gigley et al., 2009). Whether this heightened microbicidal capacity occurs by an IRG mechanism or through a separate pathway remains unknown. However, analysis of the progeny from a genetic cross between type I and III (Taylor et al., 2006), reveals that ROP18 is necessary for avoidance of *Irgb6* recruitment, even if it is not fully sufficient for survival (unpublished data). In contrast, our studies conclusively show that ROP18 is both necessary and sufficient for avoidance of IRG loading and survival in naïve, IFN- $\gamma$ -activated, and inflammatory monocytes *in vitro*. The later cell type is especially important during early infection, when Gr1<sup>+</sup> monocytes are recruited to the site of infection (Dunay et al., 2008; Mordue and Sibley, 2003; Robben et al., 2005). The ability of ROP18 expressing parasites to survive in Gr1<sup>+</sup> monocytes provides an explanation for the rapid expansion within this compartment, and this survival ability is strongly correlated with acute virulence.

Profiling of the substrate preference of ROP18 revealed a strong preference for Thr surrounded by acidic residues upstream and hydrophobic residues downstream. Substrates of ROP18 *in vivo* are likely further restricted due to its tethering on the parasite-containing vacuole membrane, a process that relies on the N-terminal domain (Labesse et al., 2009; Reese and Boothroyd, 2009). Consistent with this, ROP18 co-IPs and phosphorylates several IRGs. Mass spectrometry analysis of the sites modified by ROP18 revealed a conserved motif in SWI of IRGs that is targeted by ROP18. The SWI region of IRGs differs from other GTPases by the presence of conserved Thr residues that match the ROP18 preference. SWI plays a vital role in the binding of adaptor proteins, and mutations within this loop often affect function (Vetter and Wittinghofer, 2001). Separate studies show that ROP18 also phosphorylates analogous Thr residues within SWI of *Irga6*, thereby disrupting GTPase activity and preventing dimerization (Steinfeldt et al., in preparation). Although we have not directly evaluated the biochemical consequences of *Irgb6* phosphorylation, such modification likely alters GTPase function and oligomerization by a similar mechanism. Collectively, these studies indicate that ROP18 phosphorylates a critical Thr residue on SWI, rendering IRGs incapable of oligomerization and blocking loading onto the parasite-containing vacuole.

GTPases play a variety of essential roles in cells, and not surprisingly pathogens have repeatedly found ways to disrupt them by altering GTPase activity, via proteolytic cleavage, or by direct adenylation (Roy and Mukherjee, 2009). Additionally, the S/T kinase YpkA has previously been shown to phosphorylate a critical Ser residue in the diphosphate binding loop of the heterotrimeric G $\alpha$ q subunit, thereby altering GTP binding and affecting downstream signaling (Navarro et al., 2007). Our results extend this paradigm by showing that the parasite kinase ROP18 phosphorylates a motif in SWI that is conserved in a variety of IRGs, thus demonstrating that these host innate immunity mediators are direct targets of microbial virulence factors. Similar motifs are also found in the p65 family of guanylate

binding proteins (GBPs) (data not shown), which are implicated in pathogen control and also conserved in humans (Shenoy et al., 2008), suggesting this mechanism may be more widespread. The dramatic expansion of IRG and GBP proteins in vertebrates (Bekpen et al., 2005; Martens and Howard, 2006) parallels the recent expansion of the ROP kinase gene family in *T. gondii* (Peixoto et al., 2010), indicating that they have co-evolved in a molecular arms race pitting virulence against innate resistance.

## Supplementary Material

Refer to Web version on PubMed Central for supplementary material.

## Acknowledgments

We thank J. Howard for sharing unpublished data, G. Yap and N. Tolia for discussions, K. Tang, P. Erdmann-Gilmore, A.E. Davis and J. Nawas for technical assistance, and M. F. Cesbron-Delauw, J. Boothroyd, S. Kaufmann, and J. Coers for antibodies. Supported by grants from the NIH (AI036629, AI084243 to L.D.S.; AI57831 to G.A.T.; AI073142 to D.J.B; GM079498 to B.E.T.) and a VA Merit review grant (G.A.T.). The mass spectrometry at Washington University was supported by supported by NIH Grants P41RR000954 and UL1 RR024992 from the National Center for Research Resources. S.J.F. was partially supported by a Morse Berg Fellowship, Washington University. I.R.D. was supported by a fellowship from the DFG, Germany.

## EXPERIMENTAL PROCEDURES

### Parasite culture

Type I (i.e. GT-1) and type III (i.e. CTG Ble) strain parasites and transgenic type III parasites expressing ROP18 (clone V1, referred to as Type III + ROP18) and or a kinase-dead mutant (clone L1, referred to as Type III + ROP18 D/A) at a level similar to that in the type I strain, were grown as described previously (Taylor et al., 2006).

### Macrophage culture

Resident peritoneal macrophages were harvested from unstimulated naïve mice, Gr1<sup>+</sup> monocytes elicited from the peritoneal cavity following infection with 200 type III parasites and collection at day 4 postinfection, and bone marrow-derived macrophages (BMM) were cultured as described (Robben et al., 2004; Robben et al., 2005). RAW 264.7 cells (ATCC #TIB-71) were cultured in macrophage medium as described (Robben et al., 2004; Robben et al., 2005). Where indicated, cells were activated by treatment with 10 U/ml murine rIFN- $\gamma$  (R&D Systems) and 0.1 ng/ml LPS (Sigma-Aldrich; *E. coli* O55:B5) for 18-24 hrs before use.

### Microscopy

Samples were fixed and processed for immunofluorescence and transmission electron microscopy as described (Taylor et al., 2006; Zhao et al., 2008). For EM immunolocalization, cells were fixed in 4% paraformaldehyde and 0.05% glutaraldehyde (Polysciences Inc.) in 100 mM PIPES, 0.5mM MgCl<sub>2</sub>, pH 7.2 for 1 h at 4°C. Samples were infiltrated overnight in the cryoprotectant 2.3M sucrose, 20% polyvinyl pyrrolidone in PIPES, MgCl<sub>2</sub> at 4°C. Samples were frozen in liquid nitrogen, thawed in PBS and probed with rabbit anti-Irgb6 (Henry et al., 2009) (1:250) followed by FluoroNanogold anti-rabbit Fab (1:250) (Nanoprobes) and silver enhancement, as described previously (Nagamune et al., 2007). Samples were osmicated and processed for resin embedding as described (Taylor et al., 2006; Zhao et al., 2008).



## ***In vivo* infection and analysis**

Mice were maintained in an AAALAC accredited facility overseen by the Institutional Animal Care Committee. CD1 outbred mice (Charles River Laboratories) were infected by i.p. injection of 200 freshly egressed parasites grown in HFF cells. At intervals after infection, peritoneal cells were isolated by lavage using ice cold PBS and analyzed by cytospin and flow cytometry. For cytospin analysis, cells were fixed in 4% paraformaldehyde and stained for F4/80 using mAb HB-198 (ATCC # HB-198) conjugated to Alexa Fluor 488 and the parasite surface protein SAG1 using mAb DG52 conjugated to Alexa Fluor 594. The numbers of infected cells and extracellular parasites were determined by counting 10 fields at 40X from 3 replicates per animal. For flow cytometry analysis, cells were isolated on day 6 postinfection and analyzed as described (Dunay et al., 2008). Macrophages were stained with mAbs RB6-8C5 labeled with Pacific blue for Gr1 and A3-1 labeled with APC for F4/80. Parasites were stained with mAb DG52 against SAG1 followed by secondary goat anti-mouse IgG conjugated to Alexa Fluor 488. B cells were selectively removed from analysis based on staining with B220 labeled with APC-Cy7. A total of 100,000 peritoneal cells were analyzed in all samples to generate plots. Experiments were repeated three times with 3 mice per group.

## ***IRG recruitment and in vitro* macrophage clearance assays**

Macrophages were seeded on coverslips and infected with freshly harvested parasites, resulting in 30-50% of cells being infected at time zero. At 30 or 60 min post challenge, coverslips were fixed. Staining for Irgb6 was localized with rabbit  $\alpha$ Irgb6 (Henry et al., 2009), Irga6 was localized with mouse mAb 10D7 (Papic et al., 2008), Irgb10 was localized with rabbit  $\alpha$ Irgb10 (Coers et al., 2008) and the PV membrane was visualized by staining with either mAb  $\alpha$ GRA5 (Tg17-113) (Charif et al., 1990), or rabbit  $\alpha$ GRA7 (Dunn et al., 2008), followed by secondary antibodies conjugated to Alexa dyes. The number of Irgb6-positive vacuoles was determined by counting 10 fields at 40X from 3 replicates per condition. Separately, coverslips were fixed at either 30 min (T 0 h) post infection or after rinsing and culture for 19.5 h (T 20 h), followed by staining with mAb DG52 against SAG1 conjugated to Alexa Fluor 594. The number of infected cells was determined by counting 10 fields at 40X from 3 replicates per condition. Three replicate experiments were performed for each assay.

## **ROP18 phosphorylation site specificity**

The phosphorylation site consensus for ROP18 was using a positional scanning peptide array, containing peptides, kinase (80 ng per well) and  $\gamma$ -[<sup>32</sup>P]-ATP (50  $\mu$ M at 30  $\mu$ Ci/mL) and incubated for 2 h at 30 °C, as described (Turk et al., 2006). Aliquots were spotted onto streptavidin-coated membranes (Promega), air-dried and exposed to a phosphorimaging screen. Radiolabel incorporation into each peptide was quantified using QuantityOne software (BioRad), and the data were normalized as described (Turk et al., 2006). Phosphoblot data were normalized to adjust the values for Thr (multiplied by 0.5) and converted to a WebLogo (Crooks et al., 2004).

## **Motif analysis**

The normalized values from phosphopeptide ROP18 array were used to create a Gribskov protein profile suitable for use with “prophet” available from EMBOSS (Rice et al., 200). IRG family members (Supplemental data file 1) were searched using the ROP18 motif to determine preferred 10-letter words centered on all possible Thr residues. The top five

scoring T-words from each IRG protein were then submitted to MEME (Bailey et al., 2006) to produce sequence logos.

## Immunoprecipitation and Western blot analysis

Cells were lysed in PhosphoSafe extraction reagent (Novagen) plus protease inhibitors, as described (Qiu et al., 2008). Antibodies used for immunoprecipitation included: mAb BB2 against the Ty-tagged ROP18 (Bastin et al., 1996), rabbit  $\alpha$ Irgb6 (Henry et al., 2009), mouse mAb 5D9 against Irga6 (Zerrahn et al., 2002), and rabbit  $\alpha$ Irgb10 (Coers et al., 2008). Specificity was confirmed by MS-MS analysis. Protein G sepharose (Pierce Biotechnology Inc.) was precharged with antibodies 1 h, washed with PBS, and incubated with cell lysates overnight at 4°C., followed by washing 5 times with cold PBS.

Samples were resuspended in non-denaturing SDS sample buffer, resolved in 10% acrylamide gels, transferred to nitrocellulose and probed with  $\alpha$ Ty-1 (mAb BB2) and goat  $\alpha$ Irgb6 (A-20), (Santa Cruz Biotechnology). Blots were washed, incubated with goat  $\alpha$ mouse IgG or donkey  $\alpha$ goat IgG conjugated to HRP, and detected using ECL Plus Western blotting system (GE Healthcare) and FLA5000 phosphorimager analysis (Fuji Life Sciences).

## *In vitro* and *in vivo* $^{32}$ P labeling

For *in vitro* labeling, immunoprecipitated proteins were incubated in kinase buffer consisting of 25 mM Tris-HCl pH 7.5, 15 mM MgCl<sub>2</sub> and 2 mM MnCl<sub>2</sub>, containing 10  $\mu$ Ci of  $^{32}$ P  $\gamma$ -ATP (specific activity: 3000 Ci/mmol) (Perkin Elmer, Waltham, MA) and 33  $\mu$ M unlabelled ATP. The reaction was allowed to proceed at 30°C for 30 min. Proteins were resolved on 10% SDS-PAGE gels, dried, and imaged using a FLA5000 phosphorimager.

For *in vivo* labeling, IFN- $\gamma$ -activated BMMs were incubated with 1 mCi  $^{32}$ P orthophosphate (specific activity: 8500 Ci/mmol) (Perkin Elmer, Waltham, MA) in phosphate-free medium (Invitrogen, #11971) at 37°C, 5% CO<sub>2</sub> for 3 h. Cells were infected and treated with 100 nM Calyculin A. After 30 min, monolayers were rinsed with PBS and lysed in PhosphoSafe buffer plus protease inhibitors. Irgb6 was immunoprecipitated and bound fractions were boiled in SDS sample buffer, resolved by 10% acrylamide electrophoresis, dried, and imaged using an FLA5000 phosphorimager.

## Cloning and purification of Irgb6 and *in vitro* kinase reaction

Irgb6 was amplified by RT-PCR from cDNA derived from IFN- $\gamma$  activated mouse macrophages. The complete coding region of Irgb6 was expressed as a GST fusion protein in pGEX3 (GE Health Science). Following induction with IPTG, the protein was purified using glutathione beads according to the manufacturer's directions (Thermo Scientific). For *in vitro* kinase reactions, ROP18 was immunoprecipitated from type I parasites (~100 ng total kinase) and mixed with ~ 5  $\mu$ g of purified Irgb6 *in vitro* using the kinase assay described above with unlabeled ATP at 30°C for 4 h.

## Mass spectrometry

Recombinant ROP18 type I was expressed and purified as described previously (Qiu et al., 2008). ROP18 at 2.5 mg/ml (~60  $\mu$ M) was mixed with 1 mM ROP18S peptide – GAAPTGAIEETMK, was incubated overnight at 4°C with 2 mM MgCl<sub>2</sub> and 2 mM ATP. The sample was analyzed using an Agilent LC/MS mass spectrometer to generate ESI spectra. To locate specific sites, peptide sequencing for each peak was performed using the

MS/MS measurements on an Applied Biosystems/MDS Sciex QSTAR XL MALDI-QTOF mass spectrometer.

For identification of phosphorylation sites within full length Irgb6, the products of the *in vitro* kinase reaction described above were digested sequentially with Lys-C and trypsin and analyzed by tandem MS/MS using a linear ion trap and an Orbitrap (LTQ-Orbitrap XL, Thermo Fisher Scientific). Data were acquired using XCalibur, version 2.0.7 (Thermo Fisher). For database searches, the LC-MS files were processed using MASCOT Distiller (Matrix Science, version 2.3.0.0), as described (Nittis et al., 2010). Tandem mass spectrometry was used to acquire high (MS2) and low resolution (MS3) fragmentation spectra of tryptic peptides from Irgb6 (Supplemental Experimental Procedures).

## Generation of a $\Delta$ rop18 knockout

A knockout targeting plasmid for the *ROP18* gene (TGGT1\_063760 in www.Toxodb.org) was constructed as described in the Supplemental Experimental Procedures. Clones were isolated and genotyped using a PCR strategy as described (Fox et al., 2009) and confirmed by Western blotting of parasite lysates probed with rabbit  $\alpha$ ROP18 (Qiu et al., 2008) and rabbit  $\alpha$ TgACT1. To assess virulence, groups of five-eight CD1 mice were injected i.p. with 0.2 mL containing (100 tachyzoites) and monitored daily for survival.

## RNAi shutdown

RAW 264.7 cells were plated on glass coverslips in 24-well plates at a cell density of  $2 \times 10^5$  cells/well in macrophage medium with 10 U / mL IFN- $\gamma$  for 2 h. ON-TARGET $plus$  SMARTpool siRNA (ThermoFisher) silencing reagents were designed to target Irgb6, Irgm3 or non-targeting controls. SiRNAs were complexed with HiPerFect (Qiagen, Valencia, CA) in 100  $\mu$ l DMEM for 10 min at RT, and added to RAW246.7 cells at 50 nM. After 42-48 h post-transfection, cells were assessed for knockdown by staining with rabbit  $\alpha$ Irgb6 and phalloidin conjugated to Alexa Fluor 594. Clearance assays were performed at 42-48 h post-transfection, as described above. Mean intensity analysis was performed using Volocity software v4.0 (Improvision, Lexington, MA).

## Statistics

Statistical analyses were conducted using GraphPad (Prism). Student's *t* tests were performed under the assumption of equal variance and using a two-tailed test where a  $P \leq 0.05$  was considered significant. Mann-Whitney tests were performed and significance was calculated where  $P \leq 0.05$  was considered significant. Kaplan Meier survival analysis was performed and significance was calculated using the logrank test, where a  $P \leq 0.05$  was considered significant.

## REFERENCES

- Bailey TL, Williams NE, Misleh C, Li WW. MEME: discovering and analyzing DNA and protein sequence motifs. *Nucl Acids Res.* 2006; 34:W369–W373. [PubMed: 16845028]
- Bastin P, Bagherzadeh Z, Matthews KR, Gull K. A novel epitope tag system to study protein targeting and organelle biogenesis in *Trypanosoma brucei*. *Molec Biochem Parasitol.* 1996; 77:235–239. [PubMed: 8813669]
- Bekpen C, Hunn JP, Rohde C, Parvanova I, Guethlein L, Dunn DM, Glowalla E, Leptin M, Howard JC. The interferon-inducible p47 (IRG) GTPases in vertebrates: loss of the cell autonomous resistance mechanism in the human lineage. *Genome Biol.* 2005; 6:R92. [PubMed: 16277747]

- Charif H, Darcy F, Torpier G, Cesbron-Delauw MF, Capron A. *Toxoplasma gondii*: characterization and localization of antigens secreted from tachyzoites. *Exp Parasitol.* 1990; 71:114–124. [PubMed: 2191870]
- Coers J, Bernstein-Hanley I, Grotzky D, Parvanova I, Howard JC, Taylor GA, Dietrich WF, Starnbach MN. Chlamydia muridarum evades growth restriction by the IFN-gamma-inducible host resistance factor Irgb10. *J Immunol.* 2008; 180:6237–6245. [PubMed: 18424746]
- Crooks GE, Chandonia JM, Brenneer SE. WebLogo: a sequence logo generator. *Genome Res.* 2004; 14:1188–1190. [PubMed: 15173120]
- Dunay IR, DaMatta RA, Fux B, Presti R, Greco A, Colonna M, Sibley LD. Gr1<sup>+</sup> inflammatory monocytes are required for mucosal resistance to the pathogen *Toxoplasma gondii*. *Immunity.* 2008; 29:306–317. [PubMed: 18691912]
- Dunn JD, Ravindran S, Kim SK, Boothroyd JC. The *Toxoplasma gondii* dense granule protein GRA7 is phosphorylated upon invasion and forms an unexpected association with the rhostry proteins ROP2 and ROP4. *Infect Immun.* 2008; 76:5853–5861. [PubMed: 18809661]
- El Hajj H, Lebrun M, Arold ST, Vial H, Labesse G, Dubremetz JF. ROP18 is a rhostry kinase controlling the intracellular proliferation of *Toxoplasma gondii*. *PLoS Path.* 2007; 3:e14.
- Fox BA, Ristuccia JG, Gigley JP, Bzik DJ. Efficient gene replacements in *Toxoplasma gondii* strains deficient for nonhomologous end joining. *Eukaryot Cell.* 2009; 8:520–529. [PubMed: 19218423]
- Geissmann F, Manz MG, Jung S, Sieweke MH, Merad M, Ley K. Development of monocytes, macrophages, and dendritic cells. *Science.* 2010; 327:656–661. [PubMed: 20133564]
- Ghosh A, Uthaiyah R, Howard J, Herrmann C, Wolf E. Crystal structure of IIGP1: a paradigm for interferon-inducible p47 resistance GTPases. *Mol Cell.* 2004; 15:727–739. [PubMed: 15350217]
- Gigley JP, Fox BA, Bzik DJ. Cell-mediated immunity to *Toxoplasma gondii* develops primarily by local Th1 host immune responses in the absence of parasite replication. *J Immunol.* 2009; 182:1069–1078. [PubMed: 19124750]
- Håkansson S, Charron AJ, Sibley LD. *Toxoplasma* vacuoles: a two-step process of secretion and fusion forms the parasitophorous vacuole. *EMBO J.* 2001; 20:3132–3144. [PubMed: 11406590]
- Hanks SK, Hunter T. Protein kinases 6. The eukaryotic protein kinase superfamily: kinase (catalytic) domain structure and classification. *FASEB J.* 1995; 9:576–596. [PubMed: 7768349]
- Henry SC, Daniell XG, Burroughs AR, Indaram M, Howell DN, Coers J, Starnbach MN, Hunn JP, Howard JC, Feng CG, et al. Balance of Irgm protein activities determines IFN-gamma-induced host defense. *J Leukoc Biol.* 2009; 85:877–885. [PubMed: 19176402]
- Hunn JP, Koenen-Waisman S, Papic N, Schroeder N, Pawlowski N, Lange R, Jaiser F, Zerrahn J, Martens S, Howard JC. Regulatory interactions between IRG resistance GTPases in the cellular response to *Toxoplasma gondii*. *EMBO J.* 2008; 27:2495–2509. [PubMed: 18772884]
- Khaminets A, Hunn JP, Koenen-Waisman S, Zhao YO, Preukschat D, Coers J, Boyle JP, Ong YC, Boothroyd JC, Reichmann G, et al. Coordinated loading of IRG resistance GTPases on to the *Toxoplasma gondii* parasitophorous vacuole. *Cell Microbiol.* 2010; 12:939–961. [PubMed: 20109161]
- Khan A, Taylor S, Ajioka JW, Rosenthal BM, Sibley LD. Selection at a single locus leads to widespread expansion of *Toxoplasma gondii* lineages that are virulence in mice. *PLoS Genetics.* 2009; 5:e1000404. [PubMed: 19266027]
- Labesse G, Gelin M, Bessin Y, Lebrun M, Papoin J, Cerdan R, Arold ST, Dubremetz JF. ROP2 from *Toxoplasma gondii*: a virulence factor with a protein-kinase fold and no enzymatic activity. *Structure.* 2009; 17:139–146. [PubMed: 19141290]
- Ling YM, Shaw MH, Ayala C, Coppens I, Taylor GA, Ferguson DJP, Yap GS. Vacuolar and plasma membrane stripping and autophagic elimination of *Toxoplasma gondii* in primed effector macrophages. *J Exp Med.* 2006; 203:2063–2071. [PubMed: 16940170]
- Martens S, Howard JC. The interferon-inducible GTPases. *Annu Rev Cell Dev Biol.* 2006; 22:559–589. [PubMed: 16824009]
- Martens S, Parvanova I, Zerrahn J, Griffiths G, Schell G, Reichmann G, Howard JC. Disruption of *Toxoplasma gondii* parasitophorous vacuoles by the mouse p47-resistance GTPases. *PLoS Path.* 2005; 1:e24.

- Mordue DG, Sibley LD. A novel population of Gr-1<sup>+</sup> activated macrophages induced during acute toxoplasmosis. *J Leukoc Biol.* 2003; 74:1015–1025. [PubMed: 12972511]
- Nagamune K, Beatty WL, Sibley LD. Artemisinin induces calcium-dependent secretion in *Toxoplasma gondii*. *Euk Cell.* 2007; 6:2147–2156.
- Navarro L, Koller A, Nordfelth R, Wolf-Watz H, Taylor S, Dixon JE. Identification of a molecular target for the Yersinia protein kinase A. *Mol Cell.* 2007; 26:465–477. [PubMed: 17531806]
- Nittis T, Guittat L, LeDuc RD, Dao B, Duxin JP, Rohrs H, Townsend RR, Stewart SA. Revealing novel telomere proteins using in vivo cross-linking, tandem affinity purification, and label-free quantitative LC-FTICR-MS. *Mol Cell Proteomics.* 2010; 9:1144–1156. [PubMed: 20097687]
- Papic N, Hunn JP, Pawlowski N, Zerrahn J, Howard JC. Inactive and active states of the interferon-inducible resistance GTPase, Irga6, in vivo. *J Biol Chem.* 2008; 283:32143–32151. [PubMed: 18784077]
- Peixoto L, Chen F, Harb OS, Davis PH, Beiting DP, Brownback CS, Ouluguem D, Roos DS. Integrative genomics approaches highlight a family of parasite-specific kinases that regulate host responses. *Cell Host Microbe.* 2010; 8:208–218. [PubMed: 20709297]
- Qiu W, Wernimont A, Tang K, Taylor S, Lunin V, Schapira M, Fentress SJ, Hui R, Sibley LD. Novel structural and regulatory features of rhopty secretory kinases in *Toxoplasma gondii*. *EMBO J.* 2008; 28:969–979. [PubMed: 19197235]
- Reese ML, Boothroyd JC. A helical membrane-binding domain targets the *Toxoplasma* ROP2 family to the parasitophorous vacuole. *Traffic.* 2009; 10:1458–1470. [PubMed: 19682324]
- Rice P, Longden I, Bleasby A. EMBOS: The European molecular biology open software suite. *Trends Genetics.* 16:276–277. 200.
- Robben PM, Mordue DG, Truscott SM, Takeda K, Akira S, Sibley LD. Production of IL-12 by macrophages infected with *Toxoplasma gondii* depends on the parasite genotype. *J Immunol.* 2004; 172:3686–3694. [PubMed: 15004172]
- Robben PR, LaRegina M, Kuziel WA, Sibley LD. Recruitment of Gr-1<sup>+</sup> monocytes is essential for control of acute toxoplasmosis. *J Exp Med.* 2005; 201:1761–1769. [PubMed: 15928200]
- Roy CR, Mukherjee S. Bacterial FIC Proteins AMP Up Infection. *Sci Signal.* 2009; 2:pe14. [PubMed: 19293428]
- Saeij JPJ, Boyle JP, Collier S, Taylor S, Sibley LD, Brooke-Powell ET, Ajioka JW, Boothroyd JC. Polymorphic secreted kinases are key virulence factors in toxoplasmosis. *Science.* 2006; 314:1780–1783. [PubMed: 17170306]
- Shenoy AR, Kim BH, Choi HP, Matsuzawa T, Tiwari S, MacMicking JD. Emerging themes in IFN-gamma-induced macrophage immunity by the p47 and p65 GTPase families. *Immunobiol.* 2008; 212:771–784.
- Sibley LD. Invasion strategies of intracellular parasites. *Science.* 2004; 304:248–253. [PubMed: 15073368]
- Sibley LD, Ajioka JW. Population structure of *Toxoplasma gondii*: Clonal expansion driven by infrequent recombination and selective sweeps. *Ann Rev Microbiol.* 2008; 62:329–351. [PubMed: 18544039]
- Sibley, LD.; Charron, AJ.; Hakansson, S.; Mordue, DG. Invasion and intracellular survival by *Toxoplasma*. In: Denkers, EY.; Gazzinelli, RT., editors. *Protozoans in macrophages*. Landes Bioscience; Austin: 2007. p. 16-24.
- Taylor GA, Feng CG, Sher A. Control of IFN-g mediated host resistance to intracellular pathogens by immunity-related GTPases (p47 GTPases). *Microb Infect.* 2007; 9:1644–1651.
- Taylor S, Barragan A, Su C, Fux B, Fentress SJ, Tang K, Beatty WL, Haij EL, Jerome M, Behnke MS, et al. A secreted serine-threonine kinase determines virulence in the eukaryotic pathogen *Toxoplasma gondii*. *Science.* 2006; 314:1776–1780. [PubMed: 17170305]
- Turk BE, Hutti JE, Cantley LC. Determining protein kinase substrate specificity by parallel solution-phase assay of a large number of peptide substrates. *Nat Protoc.* 2006; 1:375–379. [PubMed: 17406259]
- Vetter IR, Wittinghofer A. The guanine nucleotide-binding switch in three dimensions. *Science.* 2001; 294:1299–1304. [PubMed: 11701921]

- Yap G, Shaw MH, Ling Y, Sher A. Genetic analysis of host resistance to intracellular pathogens: lessons from studies of *Toxoplasma gondii*. *Microb Infect*. 2006; 8:1117–1118.
- Zerrahn J, Schaible UE, Brinkmann V, Guhlich U, Kaufmann SH. The IFN-inducible Golgi- and endoplasmic reticulum-associated 47-kDa GTPase IIGP is transiently expressed during listeriosis. *J Immunol*. 2002; 168:3428–3436. [PubMed: 11907101]
- Zhao Y, Ferguson DJ, Wilson DC, Howard JC, Sibley LD, Yap GS. Virulent *Toxoplasma gondii* evade immunity-related GTPase-mediated parasite vacuole disruption within primed macrophages. *J Immunol*. 2009a; 182:3775–3781. [PubMed: 19265156]
- Zhao YO, Khaminets A, Hunn JP, Howard JC. Disruption of the *Toxoplasma gondii* parasitophorous vacuole by IFN-gamma-inducible immunity-related GTPases (IRG proteins) triggers necrotic cell death. *PLoS Pathog*. 2009b; 5:e1000288. [PubMed: 19197351]
- Zhao YO, Rohde C, Lilue JT, Konen-Waisman S, Khaminets A, Hunn JP, Howard JC. *Toxoplasma gondii* and the Immunity-Related GTPase (IRG) resistance system in mice: a review. *Mem Inst Oswaldo Cruz*. 2009c; 104:234–240. [PubMed: 19430648]
- Zhao Z, Fux B, Goodwin M, Dunay IR, Strong D, Miller BC, Cadwell K, Delgado MA, Ponpuak M, Green KG, et al. Autophagosome-independent essential function for the autophagy protein Atg5 in cellular immunity to intracellular pathogens. *Cell Host Microbe*. 2008; 4:458–469. [PubMed: 18996346]

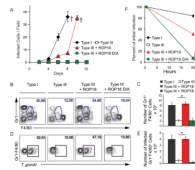


**Figure 1. ROP18 promotes growth in Gr1<sup>+</sup> inflammatory monocytes**

(A) *In vivo* parasite expansion following i.p. injection with 200 parasites. Comparison of Type I (ROP18 expressing), type III (ROP18-deficient), transgenic type III parasites expressing active type I ROP18 (Type III + ROP18) or kinase-dead ROP18 (Type III + ROP18 D/A) (Taylor et al., 2006). Mean  $\pm$  SD, n=3 animals (representative of two experiments), (†=succumbed).

(B) Flow cytometry analysis of cell recruitment to the peritoneum at 6 days postinfection. Plots from a single representative animal. Numbers indicate % Gr1<sup>+</sup> F4/80<sup>+</sup> inflammatory monocytes.

(C) Number of Gr1<sup>+</sup> F4/80<sup>+</sup> monocytes in the peritoneum at 6 days post infection. Mean  $\pm$  SD, n = 3 animals (\**P* < 0.005, Student's *t* test), representative from 3 experiments.

(D) Gr1<sup>+</sup>/F4/80<sup>+</sup> monocytes from C were gated and analyzed for infection with *T. gondii* based on staining for surface antigen 1 (SAG1). Plots represent a single representative animal. Numbers indicate % Gr1<sup>+</sup> inflammatory monocytes that were infected.

(E) Number of infected Gr1<sup>+</sup> F4/80<sup>+</sup> monocytes in the peritoneum at 6 days postinfection. Mean  $\pm$  SD, n = 3 animals (\**P* < 0.005, Student's *t* test), representative from 3 experiments.

(F) *In vitro* parasite clearance in elicited Gr1<sup>+</sup> monocytes, which were identified by surface staining. Mean  $\pm$  SEM, n=3 experiments (\*\**P* < 0.0005, Student's *t* test).

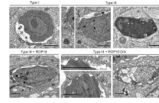


**Figure 2. ROP18 mediates protection of the parasite-containing vacuole**

Electron microscopy of parasite-containing vacuoles within Gr1<sup>+</sup> monocytes at 2 h postinfection. Type I and Type III + ROP18 parasites resided in normal vacuoles (first column), Type III and Type III + ROP18 D/A vacuoles showed vesiculation of the membrane (arrows, center column), followed by degeneration (final column). Scale=1  $\mu$ m.



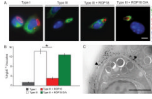


**Figure 3. ROP18 blocks Irgb6 loading**

(A) Immunofluorescence localization of Irgb6 on the parasite-containing vacuole in infected Gr1<sup>+</sup> monocytes examined at 30 min post infection. Irgb6 localized with rabbit polyclonal Ab (Alexa Fluor 488, green); GRA5 localized with mAb Tg 17-113(Alexa Fluor 594, red); and nuclei stained with DAPI (blue). Scale = 5  $\mu$ m.

(B) Quantification of Irgb6 localization to the PV in Gr1<sup>+</sup> monocytes. Mean  $\pm$  SEM, n=3 experiments (\**P* < 0.005, Student's *t* test).

(C) CryoimmunoEM localizing Irgb6 to the parasite-containing vacuole membrane (arrowheads) in macrophages. Scale = 0.5  $\mu$ m.

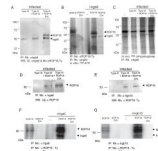


**Figure 4. ROP18 coprecipitates and phosphorylates IRGs**

(A) Immunoprecipitation (IP) of Irgb6 from macrophages infected with type III, type III expressing active ROP18 (Type III + ROP18), or type III expressing the kinase-dead form of ROP18 (Type III + ROP18 D/A). IP with specific rabbit antiserum (Rb) against Irgb6; proteins were resolved by SDS-PAGE and Western blotted with goat (Gt)  $\alpha$ Irgb6 and mouse (Mo)  $\alpha$ Ty to detect ROP18. Doublet of Irgb6 corresponds to an unknown modification.

(B) Phosphorylation of ROP18 and Irgb6 in a kinase reaction *in vitro*. Immunoprecipitated ROP18 (Mo  $\alpha$ Ty) and Irgb6 (Rb  $\alpha$ Irgb6) were incubated with  $^{32}$ P-ATP in a kinase reaction, resolved by SDS-PAGE, and signals detected by phosphorimaging. \* corresponds to Irgb6. Multiple autophosphorylation bands in ROP18 represent different processing forms as described previously (Qiu et al., 2008); the intensity of labeling characteristically changes in the presence of substrate. ROP18 migrates slightly faster in the presence of Irgb6; however, no other proteins were detected, nor modifications other than phosphorylation, were detected by MS analysis.

(C) *In vivo* phosphorylation of Irgb6 by ROP18. IFN- $\gamma$ -activated macrophages were labeled with  $^{32}$ P orthophosphate, infected for 30 min, and IP with Rb  $\alpha$ Irgb6. \* corresponds to Irgb6 as verified by MS/MS identification. Additional bands reflect contaminating host kinase activity that is unrelated to ROP18.

(D, E) IP of Irga6 (D) or Irgb10 (E) from IFN- $\gamma$ -activated macrophages with either mouse antiIrga6 (Mo  $\alpha$ Irga6) or rabbit anti-Irgb10 (Rb  $\alpha$ Irgb10) at 1 h post infection. Proteins were resolved by SDS-PAGE and blotted with rabbit anti-ROP18 (Rb  $\alpha$ ROP18) or mAb to the Ty epitope tag (Mo  $\alpha$  ROP18-Ty). Multiple bands in ROP18 represent processing as described previously (Qiu et al., 2008).

(F, G) Phosphorylation of Irga6 (F) or Irgb10 (G) by ROP18 in an *in vitro* kinase reaction. ROP18 was immunoprecipitated (IP: Mo  $\alpha$ Ty) from extracellular parasites expressing either active kinase (ROP18) or the inactive mutant (ROP18 D/A) and combined with immunoprecipitated Irga6 (IP: Mo  $\alpha$ Irga6) or Irgb10 (IP: Rb  $\alpha$ Irgb10) isolated from IFN- $\gamma$  activated macrophages. Proteins were incubated with  $^{32}$ P-ATP in a kinase reaction, resolved by SDS-PAGE, and signals detected by phosphorimaging. Multiple bands in ROP18 represent processing as described previously (Qiu et al., 2008).

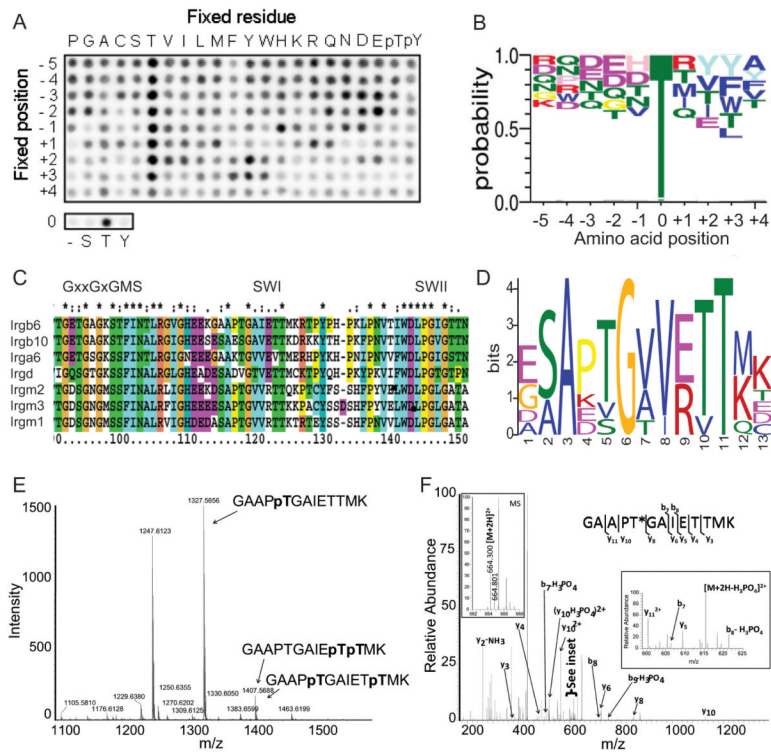


**Figure 5. ROP18 substrate preference identifies a motif in SWI of IRGs**

(A) Peptide array probing ROP18 substrate specificity by radiolabeled kinase assay.  
 (B) Sequence WebLogo of ROP18 substrate preference, phosphoacceptor site at position 0. Top five amino acids at each position are shown, height is reflective of probability.  
 (C) ClustalX alignment of select IRG proteins. Numbering based on Irgm1. SWI, switch region I; SWII, switch region II.  
 (D) MEME sequence logo of region surrounding SWI from the IRGs shown in C. Full MEME motif alignments shown in Figure S4 A,B.  
 (E) Mass spectrometry of *in vitro* phosphorylation of a peptide of Irgb6 by ROP18. MS1 spectra of unphosphorylated peptide (m/z 1247.6123), monophosphorylated, and mixed diphosphorylated peptide. Supporting data in Figure S4 C,D.  
 (F) Nano-LC-Orbitrap-MS of a tryptic phosphopeptide derived from recombinant Irgb6 incubated with ROP18. The MS2 spectrum was acquired from the  $[M+2H]^{2+}$  ion (left inset) in the Orbitrap. The high resolution CID spectrum obtained for this phosphopeptide showed a series of b and y ions that were consistent with the amino acid sequence shown (\* denotes the phosphorylated residue). Complete methods and supporting data are given in the Supplemental Information (Figure S4, Table S2).

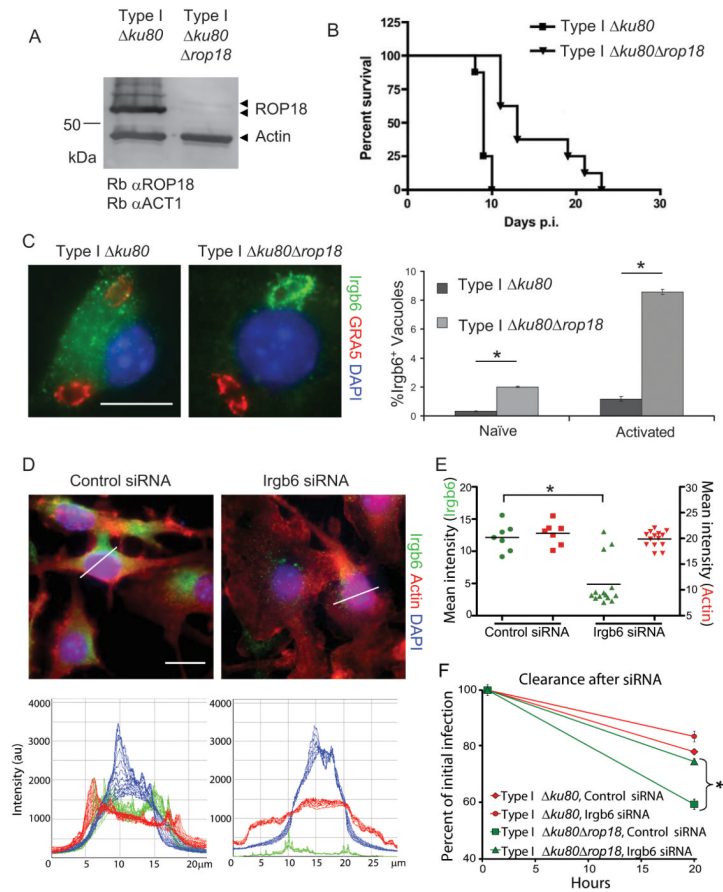


### Figure 6. ROP18 is necessary to block Irgb6 recruitment

(A) Deletion of ROP18 ( $\Delta rop18$ ) in a  $\Delta ku80$  type I strain as shown by Western blotting using rabbit anti-ROP18 (Rb  $\alpha$ ROP18) and rabbit anti-actin (Rb  $\alpha$ ACT1). Faint upper band represents processing form of ROP18 (Qiu et al., 2008).

(B) Survival of mice infected by i.p. inoculation with type I  $\Delta ku80$  strain and  $\Delta rop18$  KO. Representative of two similar experiments ( $P < 0.0001$ ),  $n = 8$  animals each.

(C) Deletion of ROP18 resulted in increased recruitment of Irgb6 in IFN- $\gamma$ -activated peritoneal macrophages at 30 min post infection. Irgb6 localized with rabbit polyclonal Ab (Alexa Fluor 488, green); GRA5 localized with mAb Tg 17-113 (Alexa Fluor 594, red); and nuclei stained with DAPI (blue). Mean  $\pm$  SEM,  $n=3$  experiments ( $*P < 0.005$ , Student's  $t$  test).

(D) Immunofluorescence staining of IFN- $\gamma$ -activated RAW 246.7 cells 48 h after addition of siRNAs targeting Irgb6 compared to control siRNA. Thin white lines indicate path for intensity profile analysis. Scale = 20  $\mu$ m. (E) Mean intensity analysis of cells treated for RNAi. Whole cell intensities were measured using Volocity software, and mean intensities for each cell were plotted. Population mean,  $*P < 0.005$ , Mann-Whitney test. (F) Enhanced clearance of  $\Delta rop18$  parasites in IFN- $\gamma$ -activated RAW 264.7 macrophages was overcome by specific depletion of Irgb6 by RNAi. Mean  $\pm$  SEM,  $n=3$  experiments,  $*P < 0.005$ , Student's  $t$  test.